Common-Mode Voltage Reduction with the Optimal PWM Signal Modulation Technique

Nguyen Nhan Bon
Faculty of Electrical and Electronics Engineering, Ho Chi Minh City University of Technology and Education, Vietnam
bonnn@hcmute.edu.vn

Thanh-Lam Le
Faculty of Electrical and Electronics Engineering, Ho Chi Minh City University of Technology and Education, Vietnam
lamlethanh@hcmute.edu.vn (corresponding author)

Received: 20 June 2024 | Revised: 28 July 2024 and 1 August 2024 | Accepted: 3 August 2024

 DOI: https://doi.org/10.48084/etasr.8193

ABSTRACT

The rapid development of electric vehicles, electric vehicle charging stations, renewable energy harvesting and storage systems, and various other energy conversion systems has increased the focus on multilevel inverters. These inverters are highly effective in reducing harmonic distortion. However, Common-Mode Voltage (CMV) remains a significant challenge, causing negative impacts, such as reduced component lifespan, decreased control system reliability, and substantial electromagnetic interference. This study introduces a straightforward and highly practical technique that ensures effective CMV reduction. The technique enhances the traditional SPWM method by offsetting the control signal to optimize switching frequency and produce better PWM signals. This method, referred to as Optimal PWM Signal Modulation (OSM), has shown superior CMV reduction capabilities for multilevel inverters compared to the phase disposition technique. The effectiveness of the OSM technique has been evaluated through simulations and practical experiments on a three-level H-bridge converter and the LAUNCHXL-F28379D development kit from Texas Instruments.

Keywords-common-mode voltage reduction; pulse width modulation; multilevel inverter; converter

I. INTRODUCTION

It is common to say that there is an increasing global movement towards clean energy. Systems integrating renewable energy sources, specifically solar and wind power, are receiving significant investment and development. In parallel, the rapid expansion of electric vehicles, their charging infrastructure, and energy storage solutions are accelerating this trend [1]. Consequently, energy conversion systems are a focal point of research and practical application. In particular, there is a growing demand for inverters, attributed to their benefits, including energy conservation, high efficiency, seamless control integration, and robust reliability [2, 3]. Among various energy conversion configurations, multilevel inverters (MLIs) are widely utilized [4, 5]. The prevalence of MLIs for high-power and high-voltage applications is steadily increasing. These MLIs are integrated with the power grid to harness renewable energy, charge electric vehicle batteries, and manage motor control systems. MLIs generate stepped output voltages with low harmonic content and can produce sinusoidal grid currents with improved power factors [6, 7]. Specifically, in a cascaded structure, the modularity of MLIs allows for flexible scaling to increase the number of levels, reduce stress on switches, enable fault-tolerant control, and ensure high reliability [8].

Although MLIs are considered advantageous in effectively reducing harmonic distortion, mitigating Common-Mode Voltage (CMV) remains a challenging issue. In motor drive applications, motors that are controlled and supplied with power from inverters may experience reduced efficiency if CMV is not effectively managed [9]. A portion of the CMV affects the shaft bearings of motors (shaft-frame voltage). The ratio of shaft voltage to CMV is typically around 10% [10]. When this peak voltage exceeds a certain threshold, bearings can fail, leading to electric discharge machining currents and subsequent bearing damage [11]. CMV and current also pose challenges for motor drive system designs due to difficulties in accurately modeling them, making the optimization of mitigation methods challenging [12, 13]. Furthermore, excessive common-mode levels can induce electromagnetic interference, causing disturbances to inverters or other electronic devices in the vicinity [14]. In electric vehicle charging systems, common-mode current and voltage are particularly significant as they can interfere with electromagnetic compatibility during wireless power transfer

processes [15]. Thus, it is evident that CMV negatively impacts component lifespan and device reliability, exacerbating harmful electromagnetic interference in motor drives.

Passive [16, 17] or active [18, 19] filters can be employed to mitigate the effects of CMV from inverters. Passive filters utilize inductors and capacitors to attenuate high-frequency components of voltage and current. Conversely, active filters typically deploy controllable devices to generate currents that cancel out common-mode currents induced by CMV. Various filter configurations and design methods have been proposed to minimize CMV and electromagnetic interference [20]. However, all these methods involve external/additional hardware, significantly increasing the cost and complexity of the energy conversion system. An alternative approach involves modifying the Pulse Width Modulation (PWM) scheme of the inverter to substantially reduce CMV at its source and mitigate its effects without additional cost [21]. Currently, several PWM techniques are employed, such as Selective Harmonic Elimination PWM (SHE-PWM), Sinusoidal PWM (SPWM), and Space Vector PWM (SVPWM) [22-24]. SVPWM necessitates computing vector components and optimal angles between vectors [25]. The SHE-PWM was introduced to reduce switching frequency by selecting pulses in a predefined voltage waveform [26]. The applicability of SHE is constrained by the number of harmonics that can be eliminated, contingent upon the selection of appropriate angles. Both methods require intricate calculations [27]. In contrast, SPWM operates differently by comparing a standard sine wave with a carrier wave to generate PWM pulses [28]. With its straightforward technique and high practical applicability, SPWM offers opportunities to control energy converters and implement advanced algorithms for reducing CMV and enhancing their output quality [27, 28].

CMV impacts present a persistent challenge in energy conversion systems. The effective CMV reduction can be achieved through software-based solutions, avoiding the need for expensive and complex hardware. This paper introduces an enhancement to the SPWM technique that significantly reduces CMV while maintaining simplicity. The proposed method, known as Optimal PWM Signal Modulation (OSM), involves offsetting the control signal by a specific amount to optimize switching frequencies and enhance PWM signal efficiency. The effectiveness of OSM is evaluated through simulations and experiments conducted on a three-level cascaded H-bridge converter. The results from these tests demonstrate that OSM provides superior CMV reduction in multilevel converters compared to the phase disposition technique, as confirmed by both simulation and practical testing scenarios.

II. THE THREE-LEVEL CASCADED H-BRIDGE INVERTER

Energy conversion systems employing multilevel cascaded H-bridge configurations commonly utilize separate DC sources as input supplies for inverters. These systems play a crucial role, especially amidst increasing demand for environmentally friendly energy solutions. With the advancement of renewable energy, electric vehicles, and microgrid systems, multilevel cascaded H-bridge inverters are gaining significant attention and widespread application. As the number of cascading levels increases, the need for independent DC sources also rises. Hence, multilevel cascaded H-bridge systems are conforming to the trend of green energy. In the schematic diagram of Figure 1, it can be observed that the Direct Current (DC) sources (denoted as E) are supplied to the branches of the H-bridge configuration. These sources can be easily found in integrated systems that contain available DC sources, such as batteries and systems directly converting energy from renewable sources. Particularly with the growing adoption of renewable energy sources, DC electrical systems are becoming integral as logical power supplies for inverters. In this study, a three-level cascaded H-bridge inverter is developed due to its modular structure facilitating easy scaling by adjusting the number of H-bridge modules, ensuring thus voltage quality, and due to its capability to achieve high power outputs. In this configuration, the IGBTs function as power switches. By selectively closing the power switches within each inverter leg per phase, voltage levels (-E, 0, E) are achieved, as detailed in Table I. This arrangement allows for precise control over the output voltage levels by modulating the switching states of the IGBTs, thereby enabling the generation of a three-level AC output waveform from a DC input source. Considering the three-phase three-level inverter in Figure 1, point O represents the neutral point of the load, while point N denotes the neutral point of the inverter. In balanced three-phase loads, the condition $V_{AO} + V_{BO} + V_{CO} = 0$ ideally holds true. However, this balance is purely theoretical and not typically achieved in practical scenarios. The voltage difference between the load neutral point and the source neutral point is termed as the CMV, which can be determined by:

$$V_{ON} = \frac{V_{AN}+V_{BN}+V_{CN}}{3} \quad (1)$$

where V_{AN}, V_{BN}, and V_{CN} represent the voltages between the output terminals of phases A, B, and C of the inverter with respect to the neutral point N, and V_{NO} denotes the CMV.

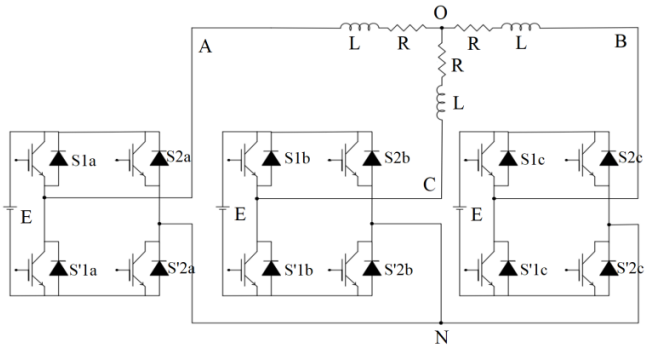

Fig. 1. Block diagram of a three-phase three-level inverter.

TABLE I. SWITCHING STATES FOR PHASE A

S_{abc}	$[S_{1a}, S_{2a}]$	Output voltage
0	[0,1]	-E
1	[0,0]; [1,1]	0
2	[1,0]	+E

With the widespread application of inverters in modern industries, issues related to CMV have posed significant

negative impacts. CMV serves as a source of shaft currents and bearing currents in motor drives, leading to mechanical damage and reduced mechanical lifespan, while also contributing to ground leakage currents in grid-connected inverters and causing electromagnetic interference. Therefore, reducing CMV is highly desirable. Both hardware and software solutions have been proposed to mitigate CMV. Software strategies based on modifying PWM have gained more attention due to their cost-effectiveness and control flexibility. In the following section, a software solution is proposed to limit CMV and improve output waveform quality for cascaded MLIs.

III. OPTIMAL PWM MODULATION FOR COMMON-MODE VOLTAGE REDUCTION

A widely used PWM technique for MLIs is the phase disposition method. This method is popular because it provides low harmonic distortion in the output voltage and current. The PWM states for a three-level inverter are represented by:

$$S_{abc} = \begin{cases} 2 \; when \; V_{dk} \geq V_{c1} \\ 1 \; when \; V_{dk} < V_{c1} \text{ or } V_{dk} \geq V_{c2} \\ 0 \; when \; V_{dk} < V_{c2} \end{cases} \quad (2)$$

where V_{dk} represents the control voltage, V_c denotes the carrier wave waveform, and S_{abc} signifies the switching states of the IGBTs or the switches in the inverter circuit.

The phase disposition method utilizes symmetric carrier waves (relative to a baseline amplitude of 1) to the reference signal. In this method, the control signal is compared with two carrier waves. When the control signal is in the positive half-cycle, it is compared with a carrier wave of amplitude (1,2). Conversely, during the negative half-cycle of the control signal, the latter is compared with a carrier wave of amplitude (0,1) as shown in Figure 2. Simulation results using MATLAB/Simulink depicting the PWM signal waveform of the phase disposition method are illustrated in Figure 2.

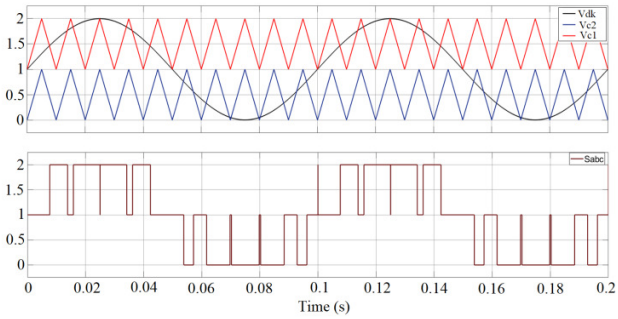

Fig. 2. Pulse modulation of the phase disposition approach.

Based on the above analysis and simulation results, it is evident that the PWM signal modulation technique using the phase disposition method produces non-optimized pulses. This is due to the comparison process involving fixed standard sine control signals and triangular waves. In this study, a simpler and more efficient method is developed to improve the output voltage quality of MLIs while reducing CMV. In the proposed OSM method, the control signal is offset by a certain V_{offset}. This adjustment normalizes the control signal, resulting in more optimal PWM pulses. This technique can also be referred to as a method utilizing modified control voltage. Each modified control voltage is derived by adding an offset voltage component V_{offset} to the control voltage of the SPWM method. The sine signal in the OSM method is defined as:

$$V_{x\text{OSM}} = V_x - V_{offset} \quad (3)$$

The offset voltage in the OSM method is determined by the average of the maximum and minimum control voltages among the control voltages at any given time. The offset voltage (V_{offset}) is calculated as:

$$V_{offset} = \frac{max(V_x)+min(V_x)}{2} \quad (4)$$

where x is the phase index, with $x = a,\ b, c$.

A comparison between the control signal based on the OSM technique and the traditional sinusoidal control signal is illustrated in Figure 3. The OSM algorithm is designed to be simple and feasible for practical applications. It is important to note that practical applications require the algorithm to be straightforward, responsive, and executable by microprocessors as quickly as possible. The control diagram of the algorithm is presented in a block diagram form in Figure 4.

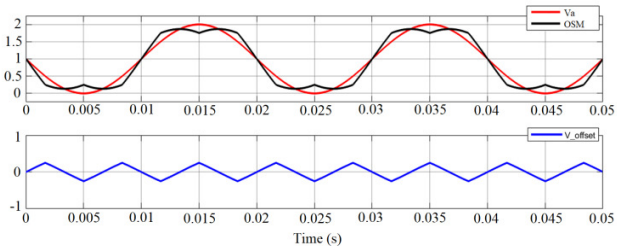

Fig. 3. Modified control waveform of the OSM method.

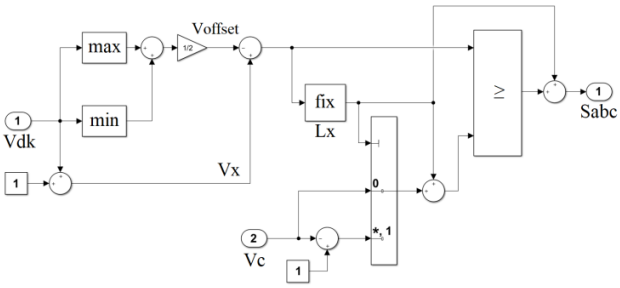

Fig. 4. Block diagram of PWM modulation with the OSM method.

IV. RESULTS AND DISCUSSION

In this section, the results of the conducted simulations and practical experiments are analyzed to verify the effectiveness of the proposed OSM method. The inverter used in this study is a three-level cascaded H-bridge type. Simulations were performed on the MATLAB/Simulink platform. The parameters for the multilevel cascaded conversion system are: sampling time 20 μs, carrier frequency 2.5 kHz, inductor 268 mH, resistor 50 Ω, and DC supply voltage V_{dc} 75 V.

A. Simulation Analysis

First, the traditional PWM generation method (Phase Disposition - PD) is conducted. The simulation results for the PD method are evidenced in Figure 5. The PD modulation method is implemented to provide a baseline for evaluating the OSM modulation method. It is noted that the modulation indices considered in this study are 0.4, 0.8, and 1, and these indices are applied to both PD and OSM methods. Figures 5 and 6 present the results for a modulation index m = 0.8. FFT analysis is performed. The Total Harmonic Distortion (THD) of the line voltage with the load is 0.78%, while the THD of the phase current is 0.85%, as measured over 10 cycles. These values are summarized in Table II. Additionally, Figure 5 presents the simulation results for the PD method, including the line voltage waveform V_{AB}, the phase voltage V_{AN}, the CMV V_{CM}, and the voltage and current across the load. The results indicate that the amplitude of the line voltage is ± 150 V, and the common-mode voltage ranges within ± 50 V (± 2 V_{dc}/3).

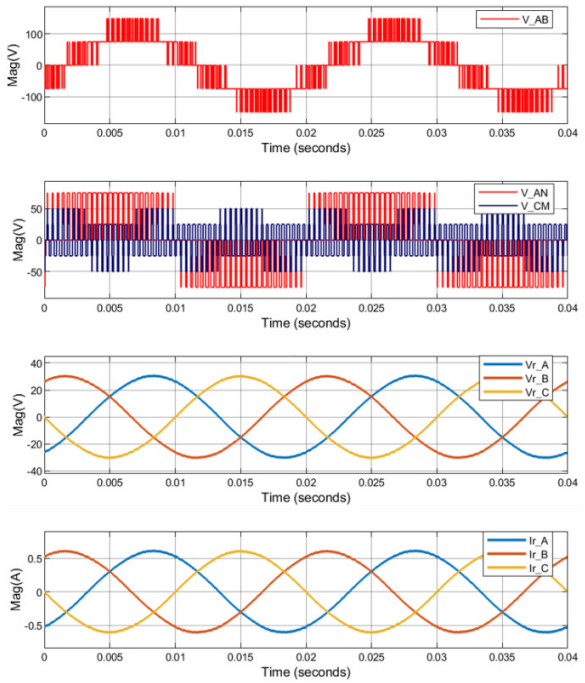

Fig. 5. Simulation results of phase disposition with m = 0.8. Waveforms of inverter output voltage and load current.

Similarly, verification simulations using the OSM method were conducted. The simulation results for the OSM method are presented in Figure 6. It can be seen that the CMV for this method has an amplitude of ± 25 V (± V_{dc}/3), which is less than half of that achieved by the PD method. Additionally, the study indicates that the harmonic distortion associated with the OSM method is higher than that of the PD method, with THD values for the line voltage and phase current being 1.76% and 1.8%, respectively. A detailed comparison of the effective CMV between the two methods is provided in Table II. This summary presents the simulation results obtained from the study. The data in Table II compare the performance of the two different methods across modulation indices ranging from 0.4 to 1. The data from Table II demonstrate that the ability of OSM to reduce CMV is superior to that of PD across all modulation indices. However, the data also show that the THD of the two methods is inversely proportional to their CMV reduction capability. Specifically, the phase disposition exhibits lower overall THD compared to OSM. Here, there is a trade-off between reducing CMV, and THD, which is acceptable as long as THD remains within acceptable limits and reducing CMV takes precedence.

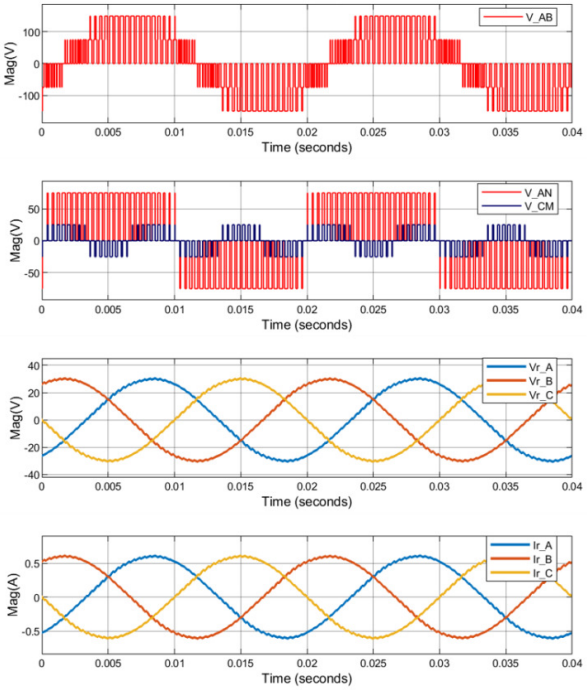

Fig. 6. Simulation results of OSM with m = 0.8. Waveforms of inverter output voltage and load current.

B. Experimental Analysis

To verify the validity of the simulation, experimental tests were also conducted. Experimental results were collected using the OWON SDS1104 oscilloscope, ensuring precise waveform analysis and reliable data acquisition. The experimental hardware setup is depicted in Figure 7. The LAUNCHXL-F28379D from Texas Instruments was utilized to execute the control program for the three-level H-bridge inverter system. The parameters utilized in the simulation are preserved and loaded into the DSP card to ensure consistency between simulation and experimentation. Moreover, this approach ensures fairness when comparing the PD and OSM methods. The algorithm was implemented on the MATLAB/Simulink software platform for both simulation and online control of the experimental model, which is a three-phase three-level cascaded H-bridge inverter using the C2000 LAUNCHXL-F28379D kit from Texas Instruments.

The experimental results with the PD method are presented in Figures 8-11. For modulation index m = 0.8, the experimental results of the PD method with line voltage V_{AB} are displayed in Figure 8.

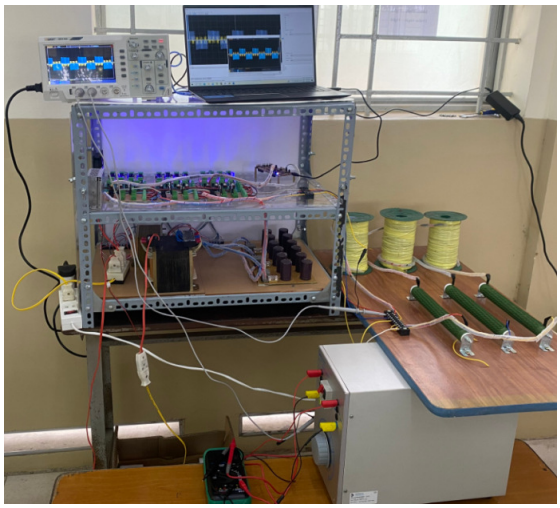

Fig. 7. Configuration of the experimental equipment.

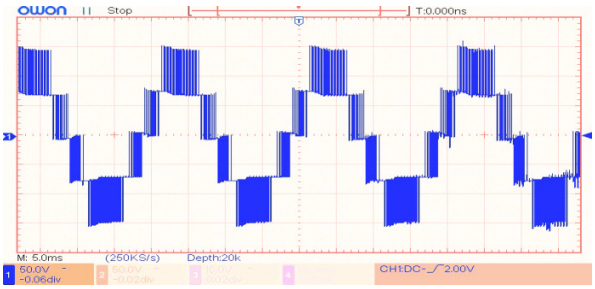

Fig. 8. Line voltage AB with phase disposition method.

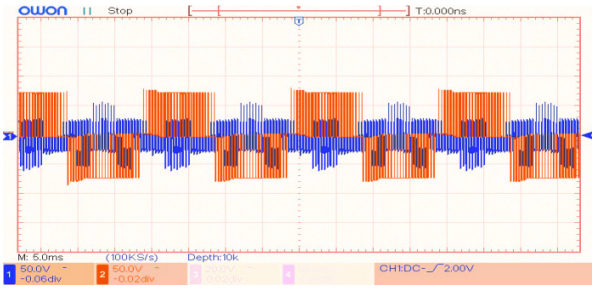

Fig. 9. Phase voltage and CMV with phase disposition method.

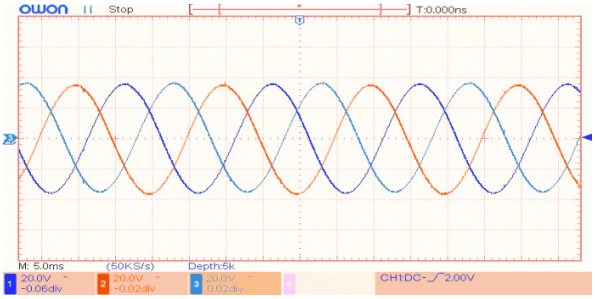

Fig. 10. Three-phase load current with phase disposition method.

The waveform of the line voltage during the PD method experiment has an amplitude of ± 150 V, consistent with the simulated waveform. The results in Figure 9 also depict waveforms of phase voltage and CMV in the phase disposition method. The CMV waveform is represented by the solid yellow line, and its amplitude ranges within ± 50 V. The three-phase current measured at the load is illustrated in Figure 10 as a standard sine wave, similar to the simulation results. The FFT analysis results of line voltage and phase current for the phase disposition method are presented in Figure 11.

(a)

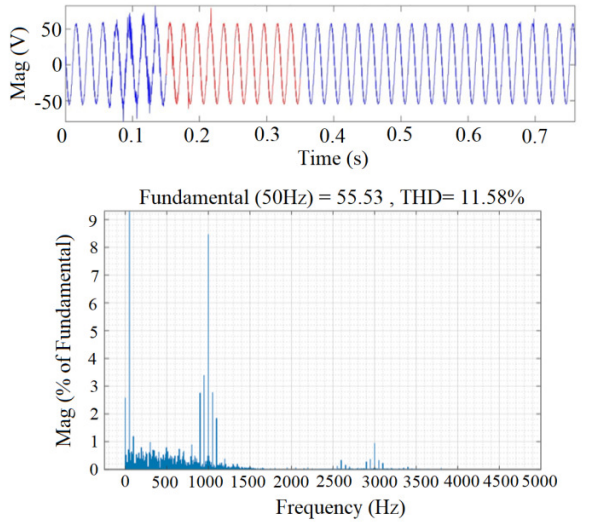

(b)

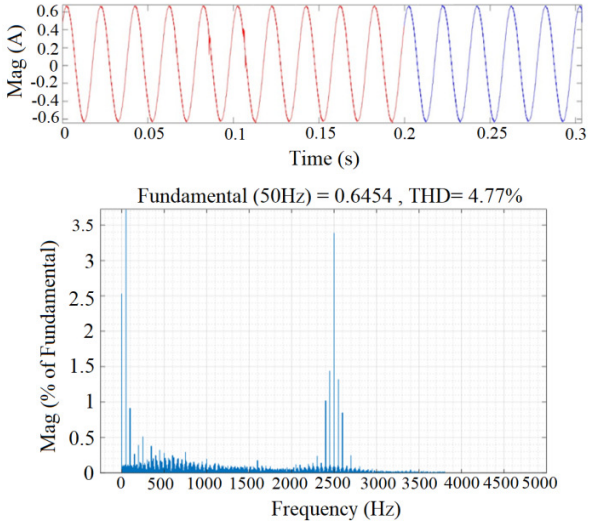

Fig. 11. Experimental FFT analysis results with phase disposition method at m = 0.8. (a) THD of line voltage, (b) THD of phase current.

The experimental results deploying the OSM method are presented in Figures 12-15 for m = 0.8. The line voltage during the experimental testing of the OSM method, as depicted in Figure 12, exhibits an amplitude of ± 150 V and a waveform similar to that of the simulation. In Figure 13, the waveforms of phase voltage and CMV in the OSM method also closely resemble the simulation results. The CMV (highlighted in yellow) manifests an amplitude within ± 25 V and includes segments where it reaches 0 volts. The three-phase current across the load, as illustrated in Figure 14, appears sinusoidal.

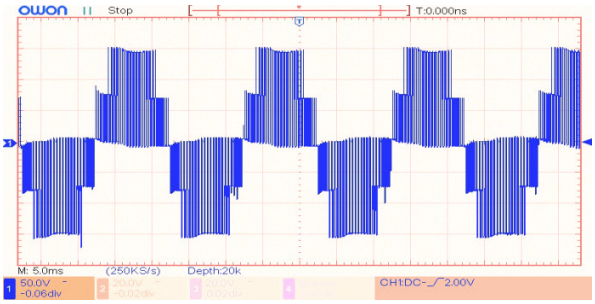

Fig. 12. Line voltage AB with OSM method.

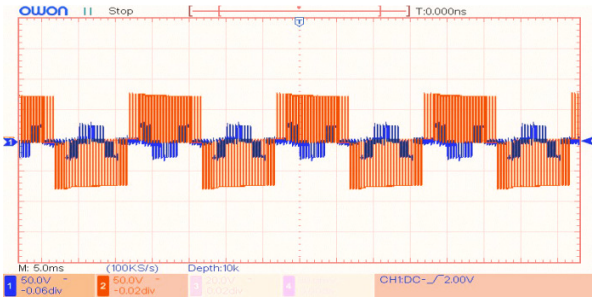

Fig. 13. Phase voltage and CMV with OSM method.

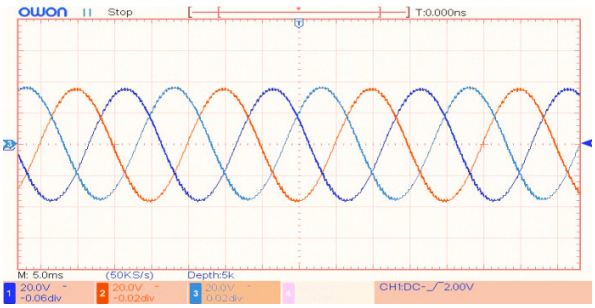

Fig. 14. Three-phase load current with OSM method.

Furthermore, an FFT analysis was conducted employing the OSM method. The results (Figure 15) indicate that the THD values of the line voltage and phase current for the OSM method are 12.05% and 5.18%, respectively. Experimental investigations with modulation indices of 0.4 and 1 were also conducted. It is evident that there is consistency between the experimental results and simulation outcomes, demonstrating the validity of the simulation process. At the same modulation index, the OSM method exhibits superior capability in reducing CMV compared to the phase disposition method. This observation underscores the effectiveness of the proposed OSM approach in practical applications, aligning closely with the theoretical predictions and the simulation results.

TABLE II. SIMULATION RESULTS OF PHASE DISPOSITION AND OSM METHODS

Parameters	Phase disposition			OSM		
m	1	0.8	0.4	1	0.8	0.4
V_{AB} **(V)**	150	150	75	150	150	150
V_{AN} **(V)**	59.71	53.24	37.19	62.12	55.01	39.83
V_{CM} **(V)**	21.12	27.97	24.28	15.61	13.83	9.81
THDu (%)	0.74	0.78	1.72	0.98	1.76	2.85
THDi (%)	0.76	0.85	1.74	0.99	1.8	2.87

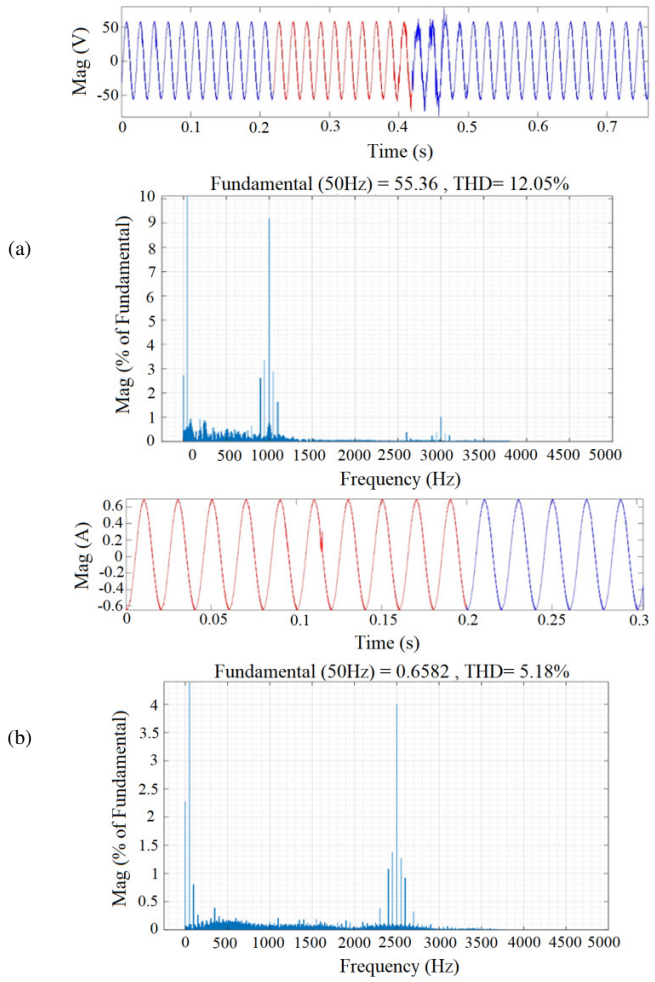

Fig. 15. Experimental FFT analysis results with OSM method at m = 0.8. (a) THD of line voltage, (b) THD of phase current.

V. CONCLUSION

Energy conversion systems are playing an increasingly critical role due to the growth of renewable energy sources, electric vehicles, and integrated small-scale power grids. However, this growth introduces challenges, particularly the common-mode voltage, which can have detrimental effects on systems involving energy converters. This study presents a straightforward and practical technique aimed at achieving common-mode reduction, named OSM. By offsetting sinusoidal control signals, the OSM technique optimizes switching frequencies and improves the quality of pulse-width modulation signals. The effectiveness of the OSM technique is assessed through simulations and experiments conducted on a three-level H-bridge converter. Results from verification tests demonstrate that OSM substantially enhances CMV reduction for multilevel inverters compared to the phase disposition technique. This enhancement is evident in both simulated scenarios and practical applications. By effectively mitigating common-mode interference, OSM not only enhances the overall output performance, but also offers a robust solution for advancing multilevel inverter systems. These findings

underscore the potential of OSM as a valuable technique in the field of energy conversion.

ACKNOWLEDGEMENT

This work is supported by the Ho Chi Minh City University of Technology and Education, under grant number: T2024-128

REFERENCES

[1] D. K. Dhaked and D. Birla, "Microgrid Designing for Electrical Two-Wheeler Charging Station Supported by Solar PV and Fuel Cell," *Indian Journal of Science and Technology*, vol. 14, no. 31, pp. 2517–2525, Jul. 2021, https://doi.org/10.17485/IJST/v14i30.224.

[2] V.-Q. Nguyen and T.-L. Le, "Flexible Control with Fuzzy Observer-Based Sliding mode for Multilevel Inverter," *Journal of Electrical Engineering & Technology*, Mar. 2024, https://doi.org/10.1007/s42835-024-01878-9.

[3] D. K. Dhaked and D. Birla, "Modeling and control of a solar-thermal dish-stirling coupled PMDC generator and battery based DC microgrid in the framework of the ENERGY NEXUS," *Energy Nexus*, vol. 5, Mar. 2022, Art. no. 100048, https://doi.org/10.1016/j.nexus.2022.100048.

[4] S. Rahman *et al.*, "Design and Implementation of Cascaded Multilevel qZSI Powered Single-Phase Induction Motor for Isolated Grid Water Pump Application," *IEEE Transactions on Industry Applications*, vol. 56, no. 2, pp. 1907–1917, Mar. 2020, https://doi.org/10.1109/TIA.2019.2959734.

[5] D. K. Dhaked, Y. Gopal, and D. Birla, "Battery Charging Optimization of Solar Energy based Telecom Sites in India," *Engineering, Technology & Applied Science Research*, vol. 9, no. 6, pp. 5041–5046, Dec. 2019, https://doi.org/10.48084/etasr.3121.

[6] T.-L. Le and M.-F. Hsieh, "An enhanced direct torque control strategy with composite controller for permanent magnet synchronous motor," *Asian Journal of Control*, vol. 26, no. 4, pp. 1683–1702, 2024, https://doi.org/10.1002/asjc.3306.

[7] B. Singh, U. Sharma, and S. Kumar, "Standalone Photovoltaic Water Pumping System Using Induction Motor Drive With Reduced Sensors," *IEEE Transactions on Industry Applications*, vol. 54, no. 4, pp. 3645–3655, Jul. 2018, https://doi.org/10.1109/TIA.2018.2825285.

[8] T.-L. Le and V.-Q. Nguyen, "A Robust Control for Five-level Inverter Based on Integral Sliding Mode Control," *International Journal of Integrated Engineering*, vol. 15, no. 4, pp. 177–192, Oct. 2023, https://doi.org/10.30880/ijie.2023.15.04.016.

[9] Y. Xu, Z. Wang, P. Liu, and J. He, "A Soft-Switching Current-Source-Inverter-Fed Motor Drive With Reduced Common-Mode Voltage," *IEEE Transactions on Industrial Electronics*, vol. 68, no. 4, pp. 3012–3021, Apr. 2021, https://doi.org/10.1109/TIE.2020.2978691.

[10] J. M. Erdman, R. J. Kerkman, D. W. Schlegel, and G. L. Skibinski, "Effect of PWM inverters on AC motor bearing currents and shaft voltages," *IEEE Transactions on Industry Applications*, vol. 32, no. 2, pp. 250–259, Mar. 1996, https://doi.org/10.1109/28.491472.

[11] S. Chen, T. A. Lipo, and D. Fitzgerald, "Modeling of motor bearing currents in PWM inverter drives," *IEEE Transactions on Industry Applications*, vol. 32, no. 6, pp. 1365–1370, Dec. 1996, https://doi.org/10.1109/28.556640.

[12] K. Rahman, A. Iqbal, N. Al-Emadi, and L. Ben-Brahim, "Common mode voltage reduction in a three-to-five phase matrix converter fed induction motor drive," *IET Power Electronics*, vol. 10, no. 7, pp. 817–825, 2017, https://doi.org/10.1049/iet-pel.2016.0661..

[13] T.-L. Le and M.-F. Hsieh, "A sliding mode-based single-loop control strategy for permanent magnet synchronous motor drives," *IET Power Electronics*, vol. 17, no. 1, pp. 78–91, 2024, https://doi.org/10.1049/pel2.12616.

[14] J.-W. Shin, C.-M. Wang, and E. M. Dede, "Power Semiconductor Module With Low-Permittivity Material to Reduce Common-Mode Electromagnetic Interference," *IEEE Transactions on Power Electronics*, vol. 33, no. 12, pp. 10027–10031, Sep. 2018, https://doi.org/10.1109/TPEL.2018.2828041.

[15] B. Strothmann, F. Schafmeister, and J. Böcker, "Common-Mode-Free Bidirectional Three-Phase PFC-Rectifier for Non-Isolated EV Charger," in *IEEE Applied Power Electronics Conference and Exposition*, Phoenix, AZ, USA, Jun. 2021, pp. 2783–2790, https://doi.org/10.1109/APEC42165.2021.9487462.

[16] V.-Q. Nguyen, M.-T. Nguyen, T.-L. Le, and N.-B. Nguyen, "Current Control for Multi-Level Inverters Based on Fuzzy Logic Sliding Mode Control Approach," in *International Conference on System Science and Engineering*, Ho Chi Minh, Vietnam, Jul. 2023, pp. 444–449, https://doi.org/10.1109/ICSSE58758.2023.10227186.

[17] Y. Liu, S. Jiang, D. Jin, and J. Peng, "Performance comparison of Si IGBT and SiC MOSFET power devices based LCL three-phase inverter with double closed-loop control," *IET Power Electronics*, vol. 12, no. 2, pp. 322–329, 2019, https://doi.org/10.1049/iet-pel.2018.5702.

[18] U. Subramaniam, S. M. Bhaskar, D. J. Almakhles, S. Padmanaban, and Z. Leonowicz, "Investigations on EMI Mitigation Techniques: Intent to Reduce Grid-Tied PV Inverter Common Mode Current and Voltage," *Energies*, vol. 12, no. 17, Jan. 2019, Art. no. 3395, https://doi.org/10.3390/en12173395.

[19] Y. Liu, Z. Mei, S. Jiang, and W. Liang, "Conducted common-mode electromagnetic interference suppression in the AC and DC sides of a grid-connected inverter," *IET Power Electronics*, vol. 13, no. 13, pp. 2926–2934, 2020, https://doi.org/10.1049/iet-pel.2019.1087.

[20] E. Robles, M. Fernandez, J. Andreu, E. Ibarra, J. Zaragoza, and U. Ugalde, "Common-mode voltage mitigation in multiphase electric motor drive systems," *Renewable and Sustainable Energy Reviews*, vol. 157, Apr. 2022, Art. no. 111971, https://doi.org/10.1016/j.rser.2021.111971.

[21] J. Huang and K. Li, "Suppression of common-mode voltage spectral peaks by using rotation reverse carriers in sinusoidal pulse width modulation three-phase inverters with CFM," *IET Power Electronics*, vol. 13, no. 6, pp. 1246–1256, 2020, https://doi.org/10.1049/iet-pel.2019.0923.

[22] T. Jing, A. Maklakov, A. Radionov, V. Gasiyarov, and Y. Liang, "Formulations, Solving Algorithms, Existing Problems and Future Challenges of Pre-Programmed PWM Techniques for High-Power AFE Converters: A Comprehensive Review," *Energies*, vol. 15, no. 5, Jan. 2022, Art. no. 1696, https://doi.org/10.3390/en15051696.

[23] S. Li, G. Song, M. Ye, W. Ren, and Q. Wei, "Multiband SHEPWM Control Technology Based on Walsh Functions," *Electronics*, vol. 9, no. 6, Jun. 2020, Art. no. 1000, https://doi.org/10.3390/electronics9061000.

[24] S. Ahmad, A. Iqbal, I. Ashraf, and M. Meraj, "Improved power quality operation of symmetrical and asymmetrical multilevel inverter using invasive weed optimization technique," *Energy Reports*, vol. 8, pp. 3323–3336, Nov. 2022, https://doi.org/10.1016/j.egyr.2022.01.122.

[25] E. Nandhini and A. Sivaprakasam, "A Review of Various Control Strategies Based on Space Vector Pulse Width Modulation for the Voltage Source Inverter," *IETE Journal of Research*, vol. 68, no. 5, pp. 3187–3201, Sep. 2022, https://doi.org/10.1080/03772063.2020.1754935.

[26] H. Behbahanifard, S. Abazari, and A. Sadoughi, "New scheme of SHE-PWM technique for cascaded multilevel inverters with regulation of DC voltage sources," *ISA Transactions*, vol. 97, pp. 44–52, Feb. 2020, https://doi.org/10.1016/j.isatra.2019.07.015.

[27] A. S. Haider, A. Naz, F. Akhter, W. Azhar, and R. Mehmood, "A Novel Efficient Sine Wave Inverter with Custom Programmed PWM and Intelligent Control," *Engineering, Technology & Applied Science Research*, vol. 6, no. 2, pp. 956–963, Apr. 2016, https://doi.org/10.48084/etasr.648.

[28] W. Boucheriette, A. Moussi, R. Mechgoug, and H. Benguesmia, "A Multilevel Inverter for Grid-Connected Photovoltaic Systems Optimized by Genetic Algorithm," *Engineering, Technology & Applied Science Research*, vol. 13, no. 2, pp. 10249–10254, Apr. 2023, https://doi.org/10.48084/etasr.5558.